

Article

Photosensitivity of Nanostructured Schottky Barriers Based on GaP for Solar Energy Applications

Vasily Rud ^{1,2,*}, Doulbay Melebaev ³, Viktor Krasnoshchekov ⁴ , Ilya Ilyin ², Eugeny Terukov ^{1,5}, Maksim Diuldin ⁴, Alexey Andreev ², Maral Shamuhammedowa ³ and Vadim Davydov ^{4,6}

¹ Ioffe Institute, 195251 St. Petersburg, Russia

² Faculty of Global Studies, M.V. Lomonosov Moscow State University, 119992 Moscow, Russia

³ Department of Physics, Turkmen State University Named for Magtymguly, Ashgabat 744000, Turkmenistan

⁴ Higher School of International Educational Program, Peter the Great Saint-Petersburg Polytechnic University, 195251 St. Petersburg, Russia

⁵ Department of Electronics, Saint Petersburg Electrotechnical University "LETI", 197022 St. Petersburg, Russia

⁶ Department of Photonics and Communication Lines, The Bonch-Bruевич Saint Petersburg State University of Telecommunication, 193232 St. Petersburg, Russia

* Correspondence: rudvas.spb@gmail.com

Abstract: This work investigates the surface-barrier photoelectric properties of Au-palladium-n-GaP structures. Research into the visible spectrum region, under the action of both linearly polarized and natural radiation, provides us with new information about the height of the barrier, the interface m-s section, and the GaP band structure. SBs based on GaP (p- and n-type) are helpful for researchers in developing advantageous structures for creating various photovoltaic devices—photodetectors for fiber-optic control of energy systems or possible structures for solar energy. Despite many years of research, issues concerning the band structure of semiconductors based on the phenomenon of photoelectroactive absorption in such surface-barrier structures' m-s remain urgent in the creation of new high-performance devices. Such structures may also be interesting for creating solar energy systems. They create a thin insulating dielectric layer (usually an oxide layer) in solar cells on SBs between the m and the semiconductor substrate. The advantage of solar cells based on m dielectric semiconductor structures is the strong electric field near the surface of the semiconductor that usually has a direction favoring the collection of carriers created by short-wavelength light. Diffusion of impurities usually results in crystal defects in the active region. There are no such defects in the studied elements. This is also the difference between solar cells on m dielectric structures and elements with diffusion in p-n junctions. We studied the PS of Au-Pd-n-GaP nanostructures to determine the height of the potential barrier $q\phi_{B0}$ and obtained accurate data on the zone structure of the n-GaP. The PS of nanostructured Au-Pd-n-GaP structures was studied in the visible region of the spectrum. Essential information about the semiconductor's potential barrier parameters and band structure was obtained. The intermediate Pd nanolayer between Au and GaP has specific effects on the Au-Pd-n-GaP nanostructure, which are of considerable practical and scientific significance for future needs.

Keywords: Schottky barrier; nanostructure; surface-barrier structures; photocurrent spectrum; spectral dependences; PS



Citation: Rud, V.; Melebaev, D.; Krasnoshchekov, V.; Ilyin, I.; Terukov, E.; Diuldin, M.; Andreev, A.; Shamuhammedowa, M.; Davydov, V. Photosensitivity of Nanostructured Schottky Barriers Based on GaP for Solar Energy Applications. *Energies* **2023**, *16*, 2319. <https://doi.org/10.3390/en16052319>

Academic Editor: James M. Gardner

Received: 29 December 2022

Revised: 21 February 2023

Accepted: 24 February 2023

Published: 28 February 2023



Copyright: © 2023 by the authors. Licensee MDPI, Basel, Switzerland. This article is an open access article distributed under the terms and conditions of the Creative Commons Attribution (CC BY) license (<https://creativecommons.org/licenses/by/4.0/>).

1. Introduction

Researchers have been concentrating for a long time on the study of Schottky barriers (SBs) based on GaP. They are interesting as structures for developing different radiation-resistant photovoltaic and electronic instruments for high-frequency power electronics, ultraviolet (UV) photoelectronics, and solar energy [1–8]. The m-s-structures with SBs based on gallium phosphide are promising in the development of UV short-wave radiation photodetectors. Such devices are easy and inexpensive to produce and robust in operation,

as the industry has mastered GaP as a wide-band-gap (high-energy-gap) semiconductor. The devices' high PS in the UV region is provided by the high threshold energy ($E_0 = 2.8$ eV, 300 K) of direct GaP optical transitions. The PS of an m-GaP structure with a Schottky barrier in the UV region ($h\nu = 3.1 \div 6.0$ eV) was studied more thoroughly than the PS in the visible light region ($h\nu = 1.5 \div 3.1$ eV). The study of the m-GaP structure visible light region provides important information on Schottky barriers and the fundamental parameters of GaP band structures.

As generally known, the Schottky barrier height ($q\varphi_{B_0}$) is a fundamental parameter of m-semiconductor (MS) and m-dielectric-semiconductor (MIS) devices used in state-of-the-art optoelectronics and microelectronics. Therein, the most accurate method for determining the $q\varphi_{B_0}$ is considered the photoelectric method (following Fowler's theory) [9,10]. With respect to a rectifying non-point MS contact, the Fowler's semi-phenomenological theory was first applied in [9–12]. Those works proposed a photovoltaic method based on measuring the PS spectra of surface-barrier structures to determine the $q\varphi_{B_0}$. In those works, a method of determining the $q\varphi_{B_0}$ for m-s structures under irradiation in the irradiation geometry from the MS junction, both from the side of the metal and from the side of the semiconductor, was offered. If the photon energy $h\nu$ was more than the height of the barrier but less than the energy-gap width of semiconductor E_g , then electron photoemission from metal to semiconductor occurred. Following Fowler's theory, the relationship between photon energy and short-circuit photocurrent I_{f0} per equal number of incident photons can be described, as in [13], at $h\nu - q\varphi_{B_0} > 3$ kT:

$$I_{f0} \sim (h\nu - q\varphi_{B_0})^2, \quad (1)$$

where T is the absolute temperature and k is the Boltzmann constant.

Therefore, photocurrent $I_{f0}^{1/2}(h\nu)$ dependence should be linear, and the extrapolation of it to the energy axis will provide values of the $q\varphi_{B_0}$. The values of the $q\varphi_{B_0}$ for Au-n-GaP structures were experimentally determined by the photoelectric method in the Fowler region of the photocurrent spectrum ($q\varphi_{B_0} < h\nu < E_g$). When the SB was irradiated from the side of a semitransparent m layer [2,13–19], the $q\varphi_{B_0}$ value at room temperature was determined within the range of $1.20 \div 1.45$ eV. The noticeable difference between these values and the $q\varphi_{B_0}$ values was explained by the influence of the intermediate layer on the diode capacitance value, since such a layer can modify the very dependence of the charge distribution in the diode on the bias. The broadband effect of PS in SBs with respect to natural light is well known [16–19]. The obtained structures show a high PS for this type of photoconverter. The PS spectra are broadband in nature, and their total width at half maximum $\delta^{1/2}$, when irradiated from the barrier contact side, is high.

Studies of obtained structures in linearly polarized radiation (LPR) showed that the polarization PS in SBs on bulk crystals and epitaxial layers, regardless of the nature of the metals used and the technological method of their deposition on the surface of isotropic semiconductors, begins to manifest itself only when the LPR beam direction deviates from the normal position to the surface of the barrier. The azimuthal dependences of the photocurrent of all barriers under conditions when the angle of incidence differs from 0° correspond to the periodic law [14], and the inequality $I_P > I_S$, which follows from the analysis of the processes of passing through the air/SB interface based on the Fresnel formulas [15], is valid in the entire PS region.

2. Materials and Methods

The surface-barrier structure is a semiconductor plate. To develop an SB, an ohmic contact is first created on a semiconductor wafer. Then, the semiconductor surface for creating the contact is prepared. A fairly clean surface area of A^{III}B^V semiconductors is obtained after etching them in a mixture of bromine (0.5 ÷ 10%) and methanol (99.5 ÷ 90%) and subsequent washing them in pure methanol [20].

An m-s barrier contact can be created by the following methods: vacuum deposition, gas-transport chemical reactions, electrochemical deposition, and chemical deposition of m [18,21–25].

The primary benefit of the chemical deposition method is the capability to easily obtain structures with properties close to the ideal model. This method creates high-quality diodes that meet today's micro- and optoelectronics requirements.

In 1971, researchers from the laboratory of Professor Dmitry Nasledov of the Ioffe Physical-Technical Institute developed a technique for metal film chemical deposition on the surface of a semiconductor to create Schottky surface-barrier diodes [26]. This technique is widely used in making various m-s diode structures. Our work was mainly aimed at improving the chemical method of Yury Goldberg [19], using the idea of nanotechnology.

The object of our study was nanostructured SB Au-Pd-n-GaP. We used [$n = (0.1 \div 5) \times 10^{17} \text{ cm}^{-3}$, $T = 300 \text{ K}$] wafers oriented in the (100) crystallographic plane with a 350–400 μm thickness, which were constructed by the Czochralski method, as an initial material for making the structures. On one GaP surface (97% In + 3% Te), ohmic contact was created. A palladium (Pd) tunnel-transparent intermediate layer 20–30 \AA thick and, then, a gold (Au) barrier contact nanolayer 100 \div 120 \AA thick, were formed on the other surface. The Pd intermediate barrier contact (BC) and layer were created by the chemical method [26,27]. A thin Pd nanolayer located between GaP and Au worked as a barrier. It improved the quality of the m-s interface and prevented diffusion of Au towards GaP. The Pd intermediate nanolayers had different thicknesses; the maximum thickness was 45 \AA . The palladium intermediate layer thickness (d) was measured using an LEM-ZM ellipsometer on a number of GaP-Pd layer structures before the formation of a barrier contact by the ellipsometric method. The chemical deposition of the Au layer at room temperature from an aqueous solution of HAuCl_4 (4 g/L) + HF (100 mL/L), according to the procedure set out in [21,23], was used to create semitransparent barrier contact. Before Au deposition or before Pd nanolayer formation, the GaP surface was treated in 4% Br_2 + 96% CH_3OH [23]. According to the ellipsometric data, the palladium intermediate layer's thickness (d) reached 20–45 \AA .

For the obtained barrier structures, the barrier contact area (S) was 0.1–1.0 cm^2 . Silver current leads of 0.05 mm in diameter were soldered to the barrier and ohmic contacts, after which capacitance-voltage characteristics (C-U) and current-voltage characteristics (I-U) were measured. We also collected information about short-circuit photocurrent spectra $I_{f0} = f(h\nu)$. All measurements were performed at $T = 300 \text{ K}$. Au-Pd-n-GaP SBs photoelectric properties were studied experimentally in two stages. In the first stage, non-polarized (natural) light irradiated the studied structures from the Au layer side (Figure 1, tap a). In the second stage, the same structures were irradiated from the same side with polarized light. The I_{f0} spectrum of the short-circuit photocurrent of the structures was measured using a DMR-4 monochromator with quartz prisms; SI 8-200 and DRT-375 lamps were used as light sources. A high PS of the SB was observed in the interval of 1 \div 2.8 eV. The absolute value of the obtained structure's quantum efficiency in the interval of $h\nu = 1 \div 5.4 \text{ eV}$ was determined using reference photodetectors calibrated in the interval of 1 \div 5.2 eV.

Based on the analysis of SBs' electric and photoelectric properties, the following GaP crystal parameters were determined: the free electron concentration $N = N_d - N_a$, the indirect (E_g , E_L), and the direct (E_0) interband transition energy. In addition, the BS energy diagram parameters were estimated: the space-charge layer width W_0 , the maximum electric field E_{m0} at the interface under zero bias, and the barrier height $q\phi_{B0}$. The direct dark current I dependence on U was also measured, which in a current densities interval of 10^{-7} – 10^{-2} A/cm^2 is exponential:

$$I = I_s \cdot e^{qU/\beta kT}, \quad (2)$$

where I_s is the saturation current.

This formula helps determine the dependence of structure ideality coefficient β on the thickness of the intermediate dielectric layer [28,29]. We used two distinct methods (photoelectric and the method of capacitance-voltage characteristics at a frequency of 10 kHz) to find the Schottky barrier's height and compared the results when $\beta < 1.3$ practically coincided (see Table 1). At this stage of the study, to determine the $q\phi_{B_0}$ and the E_0 , the PS spectra were measured in the photon energy interval $h\nu = 1.5 \div 3.2$ eV under conditions of Au-Pd-n-GaP SB irradiation from the Au side. The measured characteristic parameters of typical SBs are given in the Table 1. The volt-farad characteristics of the Au-Pd-n-GaP structures at different frequencies were measured using an E7-20 instrument. In the spectral measurements, the irradiated area of the resulting m-s junctions was ≈ 0.01 cm², and to receive equal number of incident photons, the photocurrent was reduced (Figure 2).

Table 1. Parameters of BS energy diagrams of Au-Pd-n-GaP at T = 300 K.

N_s	$S,$ cm ²	$N_d - N_a,$ cm ⁻³	$E_{m0},$ V/cm	$qU_D,$ eV	β	$q\phi_{B_0},$ eV ($I_{f0} - h\nu$)	$q\phi_B,$ eV (C - U)
1	0.230	5.6×10^{17}	4.4×10^5	1.425	1.35	1.28	1.49
2	0.197	1.1×10^{17}	2.1×10^5	1.285	1.28	1.38	1.41
3	0.165	5.9×10^{17}	4.9×10^5	1.345	1.39	1.21	1.43
4	0.110	3.8×10^{17}	3.8×10^5	1.285	1.19	1.33	1.38
5	0.123	2.6×10^{17}	3.2×10^5	1.385	1.25	1.35	1.48

Figure 1 shows typical PS spectra of Au-Pd-n-GaP BS in the spectral interval 1.5–3.2 eV when irradiated from the side of the Au nanolayers. The photocurrent of Au-Pd-n-GaP surface-barrier structures at photon energies more than the barrier height of the m-s structure ($q\phi_{B_0} = 1.3$ eV), but less than the gallium phosphide energy gap width ($E_g = 2.26$ eV), was determined by the metal–semiconductor photoemission of electrons, and at photon energies close to and greater than the energy-gap width it was determined by the nonequilibrium current carriers' excitation in the semiconductor and their separation (by the field of the surface potential barrier) [14].

The photocurrent spectrum at photon energies $q\phi_{B_0} < h\nu < E_g$ was studied in detail in this paper. It was in this spectrum window that the $q\phi_{B_0}$, a fundamental parameter of an MS structure, was determined. This parameter corresponds to the properties of Schottky diodes occurring at the MS interface. Typical spectral characteristics of Au-Pd-n-GaP structures under irradiation from the side of the Au nanolayer in the photon energy interval 1.5–2.0 eV are shown in Figure 2.

As we know, Au nanoparticles exhibit plasmonic properties, and plasmon resonance is a reason for their absorption of a light quantum [30]. Their properties strongly depend on their size. We studied the plasma resonance absorption spectrum of the Au colloidal solution by the dynamic light scattering method. It was established that plasmonic properties of nanoparticles occurred in the $\lambda = 480$ –600 nm spectral interval (where $h\nu = 2.06$ –2.58 eV). For example, the 15.27 nm Au nanoparticle diameter corresponded to the plasma resonance peak at $\lambda_m = 2525$ nm wavelength (where $h\nu = 2.36$ eV) [31]. The results indicate that as the diameter of the Au nanoparticle in the colloid decreases, the shorter wavelengths correspond to an absorption peak. Our experiments showed that the studied Au-Pd-n-GaP structures have no plasmon resonance in the Fowler spectrum region ($h\nu = 1.5$ –2.0 eV, $\lambda = 620$ –826 nm).

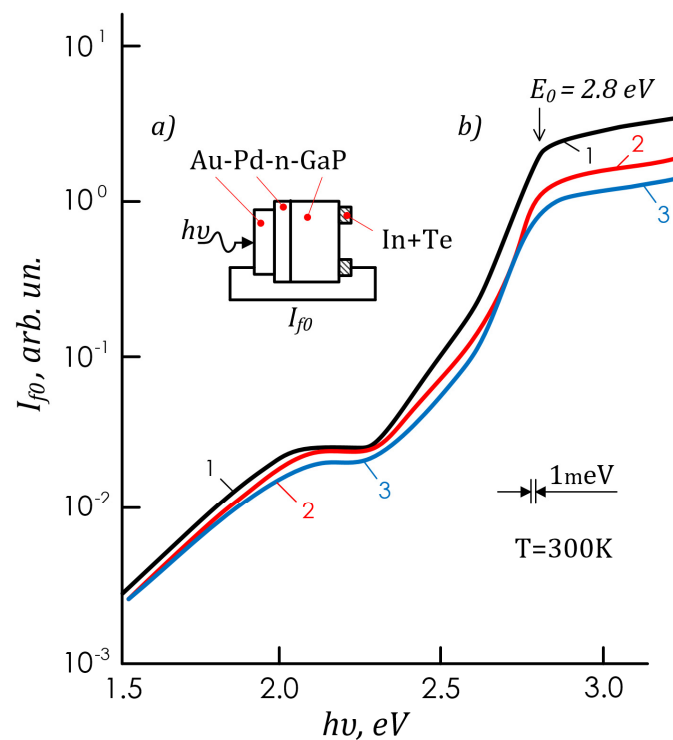


Figure 1. Diagram of a photodetector with lighting geometry (tab a); photocurrent spectra of surface-barrier structures Au-Pd-n-GaP with different thicknesses of the interlayer of palladium d. d: 1—40 Å ($\beta = 1.35$); 2—32 Å ($\beta = 1.28$); 3—45 Å ($\beta = 1.39$) (tab b). The photocurrent related to an equality of incident photons.

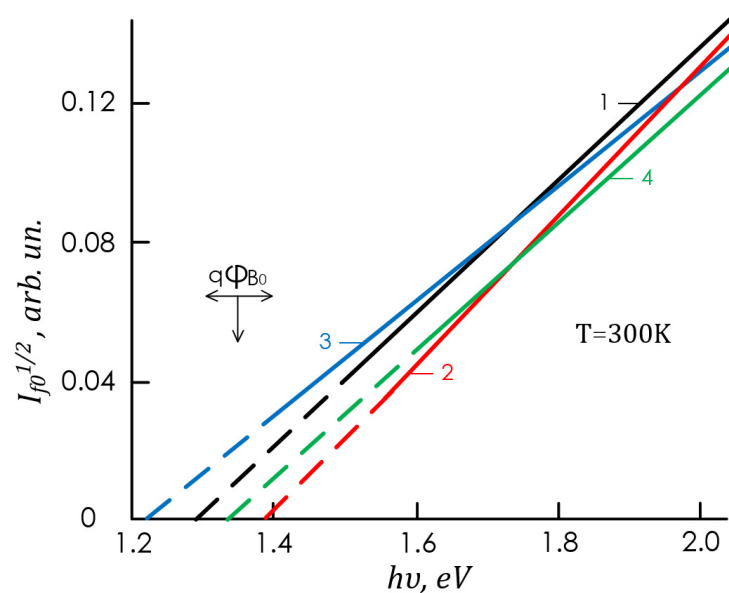


Figure 2. Dependencies of photocurrent $I_{f0}^{1/2}$ related to equality of incident photons on photon energy $h\nu$ for four Au-Pd-n-GaP surface-barrier structures with different thicknesses of the intermediate palladium layer d. d: 1—40 Å, 2—32 Å, 3—45 Å, and 4—22 Å. Here and below, we indicate sample numbers near the curves and correspond to the table.

3. Investigations of Photoelectrical Properties in Non-Polarized Light

Typical spectral characteristics of Au-Pd-n-GaP nanostructures with various Pd intermediate nanolayer thicknesses are shown in Figure 2. The $I_{f0}(h\nu)$ dependence in the interval $h\nu = 1.5\text{--}2.0$ eV obeys the Fowler law (1).

The experimental $I_{f0}^{1/2}$ dependence on $h\nu$ (Figure 2, curves 1–4) turned out to be linear. The $q\varphi_{B0}$ value was determined by extrapolating the dependence to the $I_{f0}^{1/2} = 0$. In the studied structures, this value was between 1.21–1.38 eV. For various structures, the $q\varphi_{B0}$ value was different (see the Table 1).

Figure 2 shows that the β coefficient depends on the palladium layer thickness d . The presence of a thin palladium layer ($d = 22\text{--}45$ Å; $\beta = 1.19\text{--}1.39$) between the GaP and Au at the m-s interface in the SB changed the interface properties. It caused changes in the height of the Schottky barrier (Figure 2; see the Table 1). These studies showed that by measuring the barrier height $q\varphi_{B0}$, one can obtain important information about the properties of the m-s and m-dielectric (oxide)-s interface. In the series of studies performed, it was for the first time experimentally established that the use of a thin m Pd layer with a thickness from 20 to 35 Å between a GaP and Au does not reduce the Au-n-GaP structures potential barrier height.

A good agreement with the C-U data (Figures 3–5, Table 1) was obtained for the $q\varphi_{B0}$ value of the Au-Pd-n-GaP structures in the Fowler photocurrent spectrum region ($h\nu = 1.5\text{--}2.0$ eV).

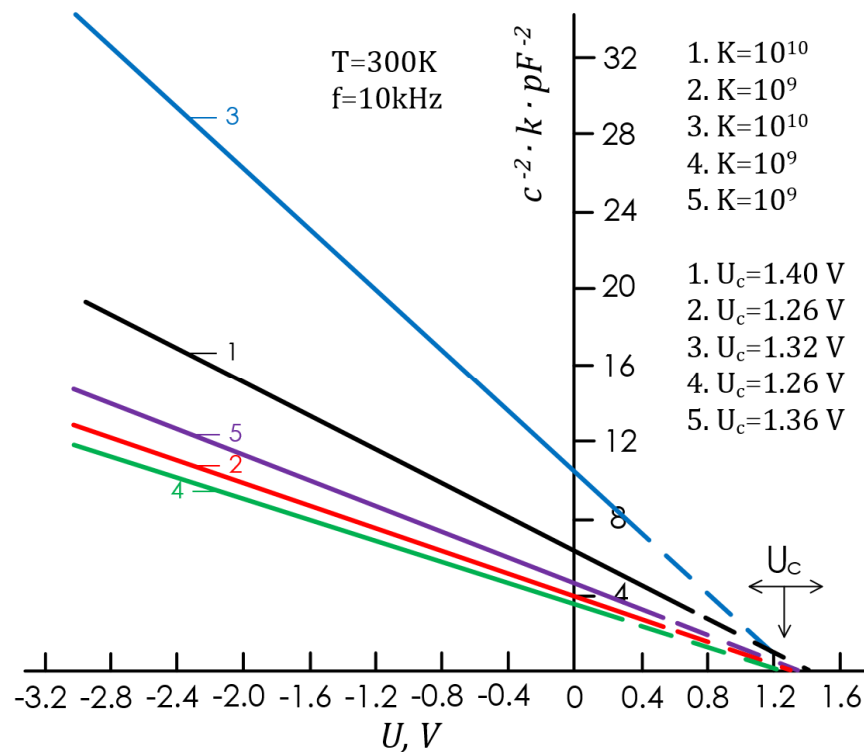


Figure 3. The differential capacitance dependence on the bias voltage of Au-Pd-n-GaP SB with various thicknesses of intermediate palladium layer d : 1—40 Å ($\beta = 1.35$); 2—32 Å ($\beta = 1.28$); 3—45 Å ($\beta = 1.39$); 4—22 Å ($\beta = 1.19$); 5—29 Å ($\beta = 1.25$).

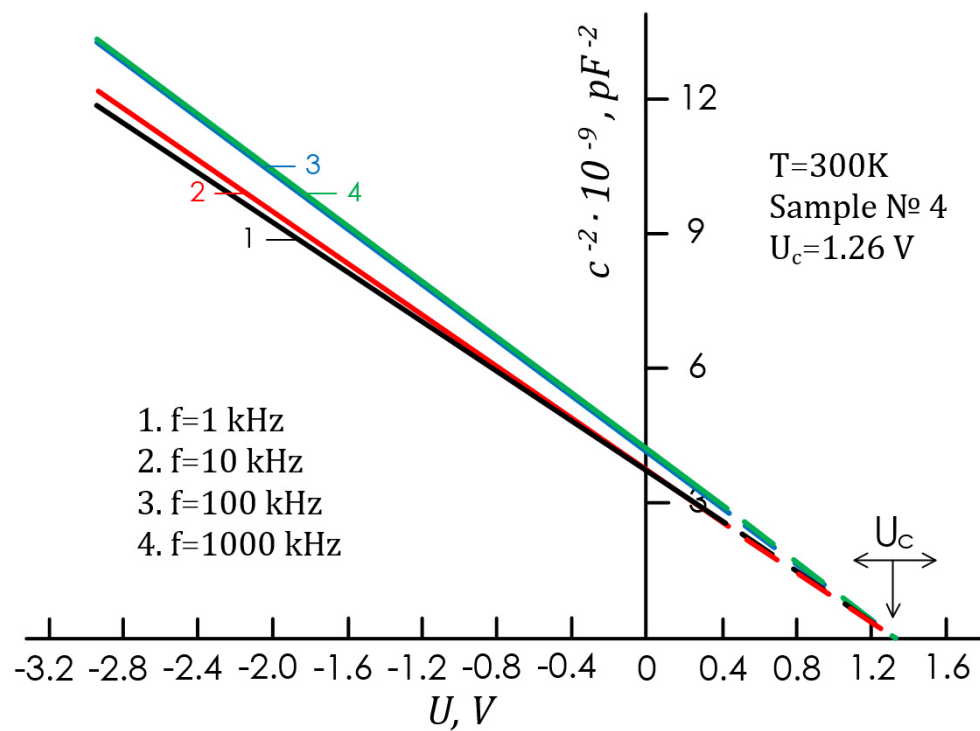


Figure 4. Differential capacitance dependence on the bias voltage for Au-Pd-n-GaP structures (Sample No. 4, $\beta = 1.19$) at different frequencies (f).

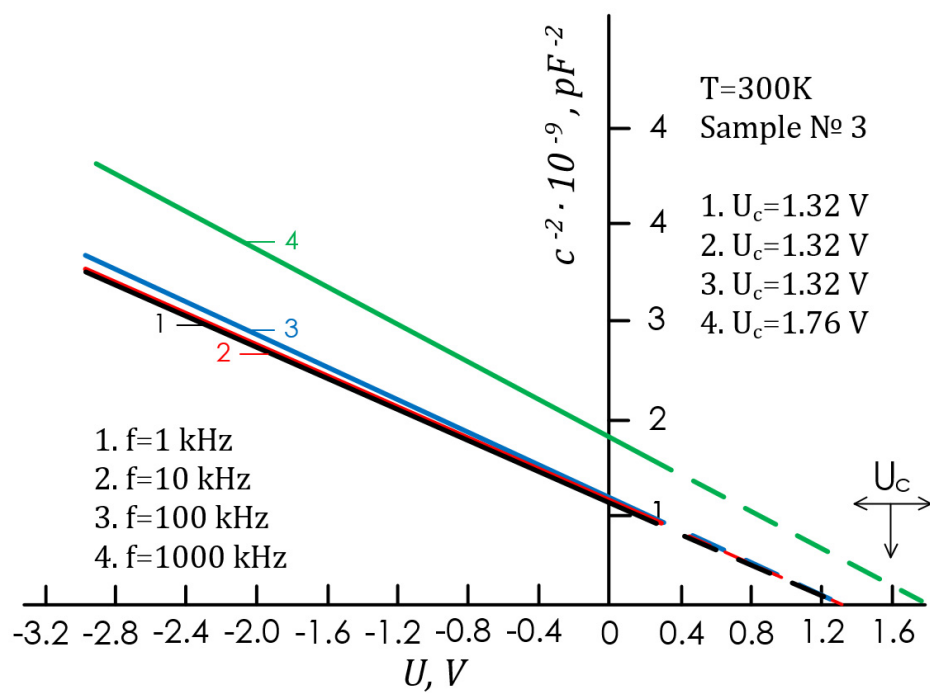


Figure 5. Differential capacitance dependence on the bias voltage for studied structures (No. 3, $\beta = 1.39$) at different frequencies (f).

The capacitance-voltage characteristics of the Au-Pd-n-GaP structures were measured. For all the studied structures, the differential barrier capacitance dependence on the voltage at the potential barrier in the coordinates $1/C^2 = f(U)$ at $U = -3.0 \div 0.4$ V obeyed a linear law (Figures 3–5), which was in agreement with Schottky theory and allowed the direct determination of the $q\phi_{B0}$ from the expression $q\phi_{B0} = qU_D - \mu = qU_C + kT - \mu$, where U is the diffusion potential, U_C is the capacitive cutoff voltage, and μ is the level energy counted from the conduction band Fermi in the GaP bulk [29–34].

At the temperature $T = 300$ K, we obtained the cutoff voltage from the intersection of the experimental dependences $C = f(U)$ with an abscissa axis for different structures of $U_0^C = U_C \approx 1.26\text{--}1.40$ V (Figure 3). For the optimal Pd intermediate layer thickness $d \approx 20\text{--}35$ Å, the $q\phi_{B0}$ values found by the two methods ($I_{f0} \sim h\nu$, $C^{-2}\text{-}U$) turned out to be practically equal (see Table 1). In Figure 4, almost ideal diodes (sample No. 4) at different frequencies ($f = 1 \div 1000$ kHz) show the observed dependence of C^{-2} on U . It was found that in an ideal diode in the $C^{-2}\text{-}U$ characteristic, the value of U_C remains constant. This means that in an almost ideal diode in a space charge layer, the internal electric field (samples No. 2, No. 4, and No. 5) does not change with frequency and the $q\phi_{B0}$ value remains unchanged. Figure 5 shows the dependence in C^{-2} coordinates on U for non-ideal diodes (No. 3, $d \approx 45$ Å; $\beta = 1.39$) at different frequencies. It was found that in non-ideal diodes of the Pd intermediate layer with $d > 35$ Å the value of U_C does not retain a constant, changing with the frequency (see Figure 5).

It was found that the average value of the Schottky barrier height was $q\phi_{B0} = 1.35$ eV (300 K) for almost ideal Au-Pd-n-GaP structures in the Fowler region (samples No. 2, No. 4, and No. 5, $h\nu = 1.5 \div 2.0$ eV). This was new received data for this diode structures, which confirmed the $I_{f0}^{1/2} \sim h\nu$ and $C^{-2}\text{-}U$ measurements. The reference literature contains $q\phi_{B0}$ data for Au-n-GaP (structures measured in different samples by different methods). We measured $I\text{-}U$, $C\text{-}U$, $I_{f0} \sim h\nu$ in the same sample using three methods. As far as we know, such a result for Au-Pd-n-GaP surface-barrier structures was obtained for the first time.

To study the band structures of GaP, Mead and Spitzer [23,25] proposed depositing a metal film on the semiconductor surface and observing the photovoltaic effect. Photoelectromotive force was proportional to optical absorption if the region was depleted of carriers and the thickness of the intermediate palladium layer d .

In the resulting transition, the diffusion length of minority carriers was much smaller than the penetration depth of light. This eliminated the difficulties of very thin samples' preparation required in light-absorption experiments. In the monograph by Sze [3] and in other works [2,14,28], it was shown that the photoelectric measurement method is the most accurate method for determining the barrier height of an m-s structure surface-barrier. Later, to determine the band parameters of both graded-gap and homo-gap semiconductors, a modernized contact photoelectric method was proposed [34–38]. The photocurrent of Au-Pd-n-GaP surface-barrier structures at photon energy $h\nu = 2.2 \div 2.8$ eV reflected the gallium phosphide band structure properties (Figures 6–8).

In the visible-light region, the photocurrent in the $h\nu = 2.3\text{--}2.65$ eV interval was due to electron transitions from the valence band to the X valley of the conduction band, while the photocurrent in the $h\nu > 2.65$ eV interval was due to electron transitions from the valence band to the "G" valley of the conduction band ($E_0 = 2.8$ eV) and was located in the violet and ultraviolet regions (Figures 6–8).

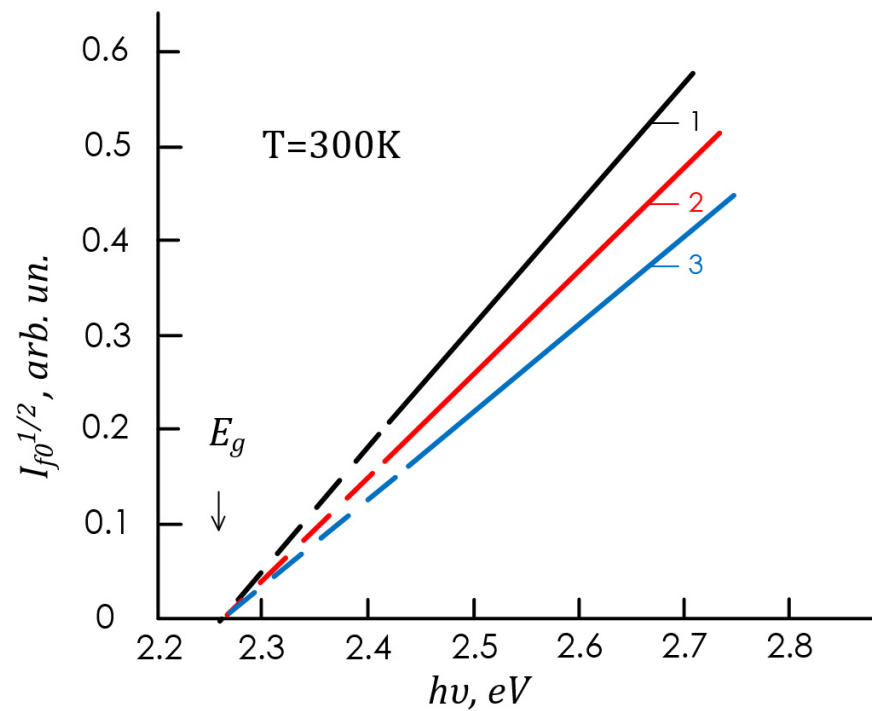


Figure 6. Dependence of the photocurrent $I_{f0}^{1/2}$ related to equality of incident photons on the $h\nu$ for three Au-Pd-n-GaP surface-barrier structures with different d : 1—40 Å, 2—32 Å, 3—45 Å.

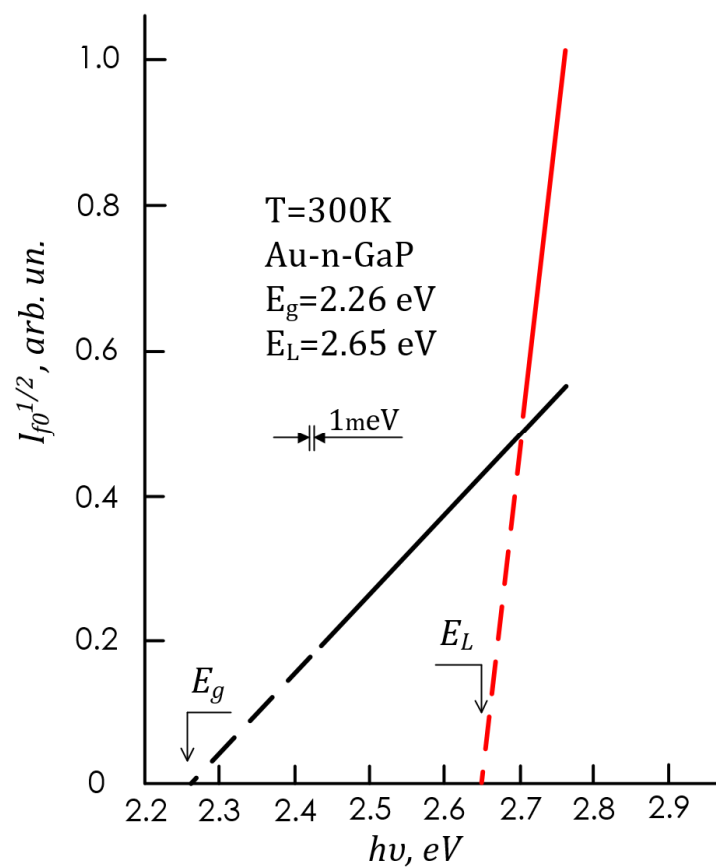


Figure 7. Dependence of the photocurrent $I_{f0}^{1/2}$ related to an equality of incident photons on the $h\nu$ for four Au-Pd-n-GaP surface-barrier structures (Sample No. 4, $\beta = 1.19$).

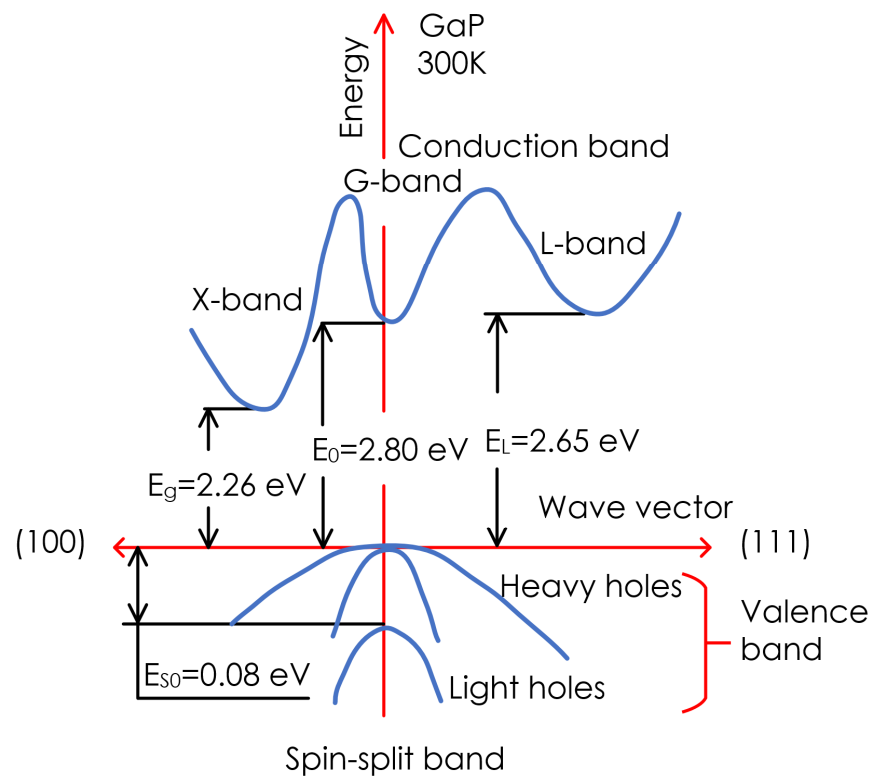


Figure 8. Scheme of optical transitions in the gallium phosphide band structure. E_g , E_0 , and E_L are energies of optical transitions determined from the photocurrent spectrum of SBs.

When analyzing the experimental dependence of I_{f0} on $h\nu$ (Figure 1, b) using the Spitzer and Mead method [11]: $I_{f0} \sim (h\nu - E_g)^2$, where $h\nu < E_0$, E_g was determined; for GaP, it was 2.26 eV at 300 K (Figure 6). To determine the threshold energy of direct optical transitions for GaP, a modernized photoelectric method was used [36]. By comparing the absorption spectrum of GaP [38–40] with the photocurrent spectra of Au-Pd-n-GaP structures in the ultraviolet regions, it was established (Figure 1, b and Figures 9 and 10) that the photocurrent I_{f0} in m-s structures at $h\nu < E_0$ usually increases exponentially with $h\nu$, and at $h\nu > E_0$ it increases first linearly and then sublinearly. The linear section begins at $h\nu = E_0$, which allows one to determine E_0 directly from the photocurrent spectrum I_{f0} of the m-s structure when the m-s junction is irradiated through the Au nanolayer, both under natural (Figure 1, b) and polarized (Figure 10) radiation. The E_0 for GaP was determined by this method; it was 2.80 eV at 300 K.

4. Investigation of PS in Linearly Polarized Light

The basic results of the performed polarization studies are presented in Figures 9–11. The regularities of photocurrent polarization measurements are as follows. When the LP light ($\Theta \neq 0^\circ$) falls from the side of Au, a broadband polarimetric effect arises in the GAP structures. In the region of the spectrum under study, the photocurrent of the structures depends on the azimuthal angle between the light wave electric vector \vec{E} and the incidence plane.

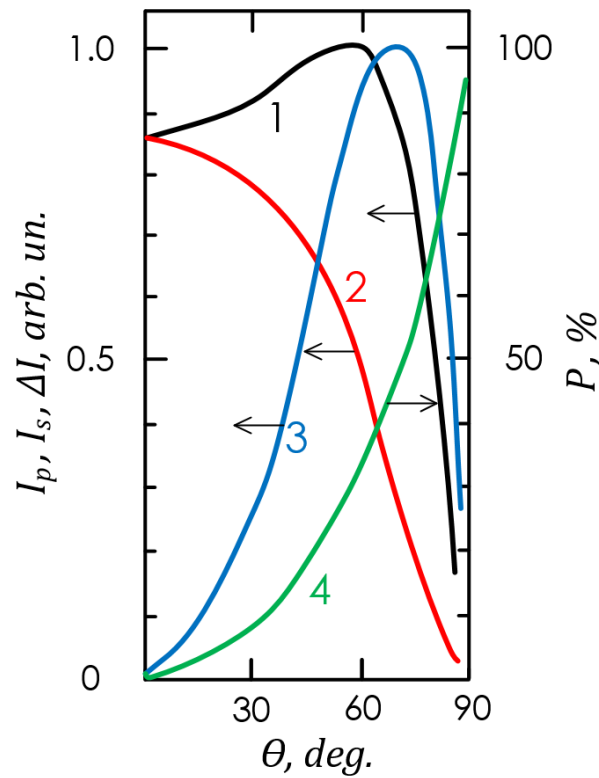


Figure 9. Dependences of photocurrents (1 corresponds I_p , 2 corresponds I_s , 3 corresponds $\Delta I = I_p - I_s$) and PPL coefficient (4 corresponds $P = \frac{\Delta I}{I_p - I_s} \cdot 100\%$) for surface-barrier structures (Sample No. 5) on the angle of incidence of linearly polarized radiation ($\lambda = 0.437 \mu\text{m}$, illumination is from the side of the barrier contact, $T = 300 \text{ K}$).

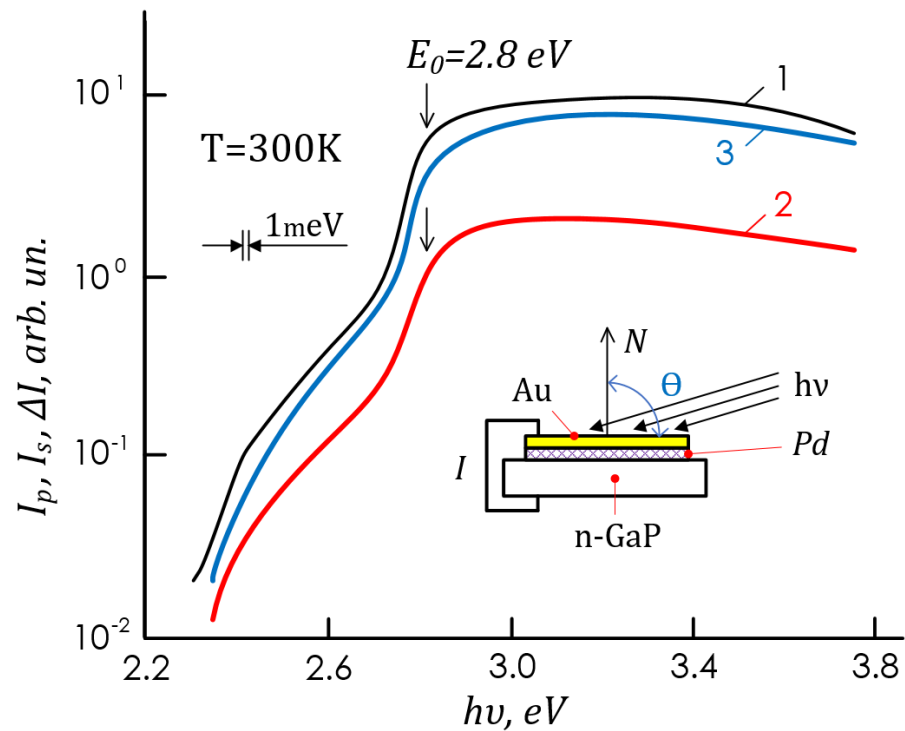


Figure 10. Spectral dependences of short-circuit photocurrent I^{\parallel} (1), photocurrent polarization difference (2), short-circuit photocurrent I^{\perp} (3), for surface-barrier structures (Sample No. 5). The inset shows the scheme of the experiment, $\Theta = 80^\circ$.

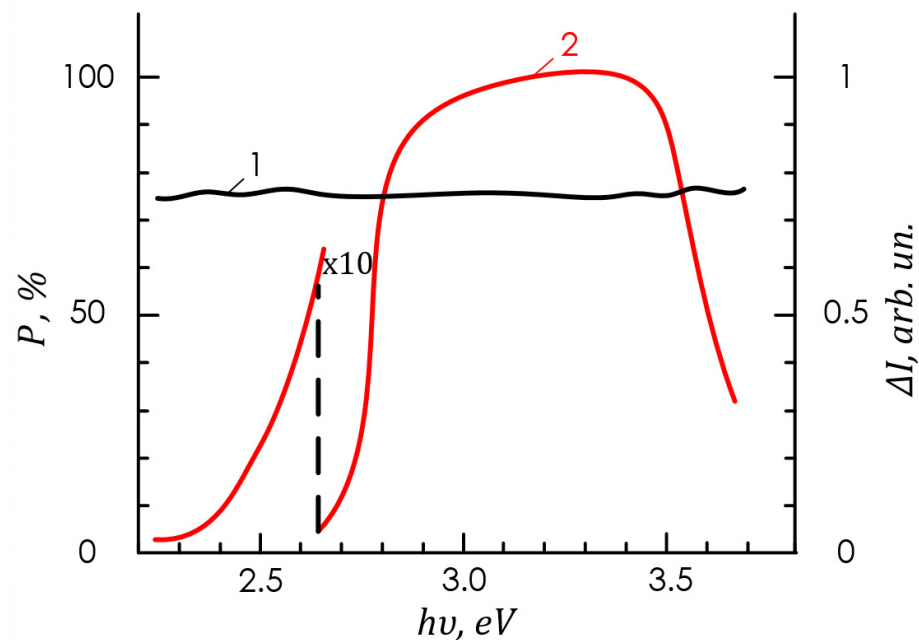


Figure 11. Spectral dependences of the PPL coefficient (1) and the polarization difference of photocurrents (2) of Au-Pd-n-GaP surface-barrier structures (Sample No 5, $T = 300$ K, $\Theta = 80^\circ$).

Figure 9 presents the dependences of the photocurrents (1— I_p , 2— I_s , 3— $\Delta I = I_p - I_s$) and the coefficient of induced PPL (4— $P = \frac{\Delta I}{I_p - I_s} \cdot 100\%$) on the angle of incidence of radiation Θ to the RP of the structures (the photocurrent I_p and I_s correspond to the irradiation of the structures when RP parallel or perpendicular to \vec{E}). For example, if the structures were illuminated with light with $\vec{E} \parallel$ RP polarization, the photocurrent I_p with increasing Θ increases at first, as can be seen from Figure 9, reaching a maximum in the vicinity of $\Theta \approx 60^\circ$, then decreases quickly.

It should be emphasized that the increase in I_p with increases in the Θ angle is due to a decrease in reflection losses from the Au surface and takes place only at E//PR. Our studies showed that the increasing IP effect is related to both the interface and Au layer surface quality. For best-quality structures, $I_{\Theta=60}/I_{\Theta=0} = 1.3$. For lower-quality structures, the dependence $I_p(\Theta)$ resembles $I_s(\Theta)$ (Figure 9) and I_s -curve 2 (Figure 10), i.e., upon increasing the photocurrent effect, I_p disappears. The analysis of the $I_p(\Theta)$ and $I_s(\Theta)$ experimental dependences should take into account the above regularities, and they are useful for controlling metal layer deposition quality on semiconductor surfaces and m-s interface quality.

Figure 10 shows the induced PPL spectral dependence in typical SB structures at angles of incidence $\Theta = 80^\circ$. The features of the studied structures connected with the long-wave photocurrent edge of I_p and I_s . According to the dependences of the polarization photocurrent I_p on $h\nu$ and I_s on $h\nu$, the E_g and E_0 for GaP were determined using the well-known method [35–39]. The maximum value of the polarization difference of photocurrents ΔI (Figure 9, curve 3) in the obtained Au-GaP structures was achieved at angles of $\Theta = 70^\circ$. At $\Theta = 0^\circ$, following the selection rules for interband optical transitions in GaP [39], the polarization difference of photocurrents ΔI , and the PPL coefficient $P = [\Delta I / (I_p + I_s)]$, 100% of the studied structures turned out to be equal to zero, i.e., there was no PS to polarization. With an increase in Θ , the PPL coefficient increased according to the law $P \sim \Theta^2$, in accordance with [26,35]. The maximum value $P = 74\%$ was reached at $\Theta = 80^\circ$ and, according to [26], corresponded to the refractive index $n = 3.2$ characteristic of GaP [39].

Spectral dependences of polarization parameters for a typical structure at $\Theta = 80^\circ$ are shown in Figure 11. The main regularity of these studies—the nonselective nature of the PPL coefficient—was observed in the entire PS region, which corresponded to the results of

the analysis [35,38]. In a wide range of incident photon energies of $2.3 \div 3.7$ eV, the obtained structures had a constant value of P , which could be quickly controlled by choosing the value of Θ (Figure 9, curve 4). The polarization difference ΔI (Figure 11, curve 2) had a spectral contour corresponding to the spectral dependence of the photocurrent of these structures in unpolarized radiation. The maximum value of ΔI fell on the fundamental absorption region of GaP and was realized for the obtained structures in the interval $2.9 \div 3.4$ eV. Since the maximum azimuthal PS of a polarimetric photodetector is $\Phi_i \sim \Delta I$ [35], it was obvious that the obtained structures could be used as photoanalyzers in the wavelength interval $0.36 \div 0.42$ μm for use in energy systems. The maximum value of the azimuthal PS of Au-GaP structures was $\Phi_i = 0.2 \div 0.21$ A/W·deg at $T = 300$ K.

5. Conclusions

A comprehensive detailed study of the GaP surface-barrier structures based on Au with palladium intermediate layer showed that, upon the formation of high-quality interface, the GaP surface stabilized and, in this case, the potential barrier height tended to a value of 1.35 eV at 300 K.

A thin palladium layer ($d < 40$ Å) performed two functions in the studied GaP surface-barrier structures. First, this tunnel-transparent intermediate nanolayer made the GaP surfaces chemically stable. Second, it prevented gold atoms' movement to the semiconductor, providing a high-quality, stable interface with the GaP semiconductor.

Investigation of PS in the visible region provided valuable information about semiconductor band structure parameters and the potential barrier. For the first time, it was experimentally established that the presence between GaP and Au of a thin metallic Pd layer with a thickness of 20 to 35 Å does not reduce the potential barrier height of the Au-n-GaP structures.

Thus, an intermediate palladium nanolayer between GaP and Au with a thickness of 20–30 Å forms specific effects in the Au-Pd-n-GaP nanostructure, which are of considerable practical and scientific significance for future needs.

Author Contributions: Conceptualization, V.R., E.T. and D.M.; methodology, V.R. and D.M.; software, V.K., M.S. and A.A.; validation, M.D.; formal analysis, V.K.; investigation, V.R. and I.I.; resources, V.R. and I.I.; data curation, V.K. and M.D.; writing—original draft preparation, V.R. and M.D.; writing—review and editing, M.D. and V.K.; visualization, M.D. and V.D.; supervision, V.R.; project administration, V.K. and E.T. All authors have read and agreed to the published version of the manuscript.

Funding: The research was partially funded by the Ministry of Science and Higher Education of the Russian Federation under the strategic academic leadership program “Priority 2030” (agreement 075-15-2021-1333, dated 30 September 2021).

Data Availability Statement: Not applicable.

Conflicts of Interest: The authors declare no conflict of interest.

Abbreviations

SB	Schottky barriers
PS	photosensitivity
PPL	photopleochroism
UV	ultraviolet
m	metal
s	semiconductor
$q\varphi_{B0}$	Schottky barrier height
E_g	width of forbidden band
I_{f0}	short circuit photocurrent

T	absolute temperature
BC	barrier contact
I_s	saturation current
β	the structure ideality coefficient
U_D	diffusion potential
U_C	capacitive cutoff voltage
\ominus	angle of incidence of radiation
P	coefficient of photopleochroism
Φ_i	azimuthal photosensitivity of a polarimetric detector
RP	receiving plane

References

- Nannichi, V.; Pearson, G.L. Properties of GaP Schottky barrier diodes at elevated temperatures. *Solid-State Electron.* **1969**, *12*, 341–348. [\[CrossRef\]](#)
- Khvostikov, V.P.; Sorokina, S.V.; Khvostikova, O.A.; Nakhimovich, M.V.; Shvarts, M.Z. GaSb-Based Thermophotovoltaic Converters of IR Selective Emitter Radiation. *Semiconductors* **2021**, *55*, 840–843. [\[CrossRef\]](#)
- Sze, S.M.; Kwok, K.; Ng, K.K. *Physics of Semiconductor Devices*, 3rd ed.; John Wiley & Sons, Inc.: New York, NY, USA, 2007; p. 815.
- Sorokina, S.V.; Soldatenkov, F.Y.; Potapovich, N.S.; Shvarts, M.Z.; Khvostikov, V.P. Au- and Ag-Containing Contacts to GaSb-Photovoltaic Converters. *IEEE Electron. Device Lett.* **2022**, *43*, 418–421. [\[CrossRef\]](#)
- Salamov, I.; Bobyl, A.; Mekhilef, S. The efficiency of the on-grid solar power plant in the Chechen Republic. *IOP Conf. Ser. Earth Environ. Sci.* **2020**, *578*, 012044. [\[CrossRef\]](#)
- Ken, O.S.; Zhukov, E.A.; Akimov, I.A.; Korenev, V.L.; Kopteva, N.E.; Kalitukha, I.V.; Sapega, V.F.; Wieck, A.D.; Ludwig, A.; Schott, R.; et al. Effect of electric current on the optical orientation of interface electrons in AlGaAs/GaAs heterostructures. *Phys. Rev. B* **2020**, *102*, 045302. [\[CrossRef\]](#)
- Nekrasov, S.V.; Akimov, I.A.; Kusrayev, Y.G.; Yakovlev, D.R.; Bayer, M. Effect of nuclear quadrupole interaction on spin beats in photoluminescence polarization dynamics of charged excitons in InP/(In,Ga)P quantum dots. *Phys. Rev. B* **2019**, *100*, 235415. [\[CrossRef\]](#)
- Bodnar', I.V.; Osipova, M.A.; Rud', V.Y.; Rud', Y.V.; Bairamov, B.K. Photoelectric properties of In/CdP₂ surface barrier structures. *J. Appl. Spectrosc.* **2010**, *77*, 148–151. [\[CrossRef\]](#)
- Lubyankina, E.A.; Toporov, V.V.; Mizerov, A.M.; Timoshnev, S.N.; Shubina, K.Y.; Bairamov, B.H.; Bouravleuv, A.D. Raman Spectroscopy of GaN Epitaxial Layers Synthesized on Si(111) by Molecular Beam Epitaxy with Nitridation. *Semiconductors* **2020**, *54*, 1847–1849. [\[CrossRef\]](#)
- Cowley, M.; Heffner, H. Gallium Phosphide-Gold Surface Barrier. *J. Appl. Phys.* **1964**, *35*, 255–256. [\[CrossRef\]](#)
- Mead, C.A. Metal-semiconductor surface barriers. *Solid-State Electron.* **1966**, *9*, 1023–1033. [\[CrossRef\]](#)
- Smith, B.L. Near ideal Au-GaP Schottky diodes. *J. Appl. Phys.* **1969**, *40*, 4675–4676. [\[CrossRef\]](#)
- White, H.G.; Logan, R.A. GaP surface-barrier diodes. *J. Appl. Phys.* **1963**, *34*, 1990–1997. [\[CrossRef\]](#)
- Goldberg, Y.A.; Posse, E.A.; Tsarencov, B.V. Ideal GaP surface—Barrier diodes. *Electron. Lett.* **1971**, *7*, 601–602. [\[CrossRef\]](#)
- Kesamanly, F.P.; Rud', V.Y.; Rud', Y.V. Induced photopleochroism in semiconductors Review. *Semiconductors* **1999**, *33*, 483–503. [\[CrossRef\]](#)
- Brillson, L.J.; Viturro, R.E.; Slade, M.L.; Chiarada, P.; Kilday, D.; Kelly, M.K.; Margaritondo, G. Near-ideal Schottky barrier formation at metal—GaP interfaces. *Appl. Phys. Lett.* **1987**, *50*, 1379–1381. [\[CrossRef\]](#)
- Sullivan, M.V.; Kolb, G.A. Chemical polishing of GaAs in bromine and methanol mixture. *J. Electrochem. Soc.* **1963**, *110*, 585–587. [\[CrossRef\]](#)
- Etmers, G.W.; Stevens, E.H. Properties of Co-GaAs, Ni-GaAs diodes fabricated by electroless plating. *Solid-State Electr.* **1972**, *15*, 721–727. [\[CrossRef\]](#)
- Goldberg, Y.A. Semiconductor near-ultraviolet photoelectronics. *Semicond. Sci. Technol.* **1999**, *14*, R41. [\[CrossRef\]](#)
- Konnikov, S.G.; Rud, V.Y.; Rud, Y.V.; Melebaev, D.; Berkeliev, A.; Serginov, M.; Tilevov, S. Photopleochroism of GaP_xAs_{1-x} Surface-Barrier Structures. *Jpn. J. Appl. Phys.* **1993**, *32*, 515–517. [\[CrossRef\]](#)
- Moulin, E.; Luo, P.; Pieters, B.; Sukmanowski, J.; Kirchhoff, J.; Reetz, W.; Müller, T.; Carius, R.; Royer, F.X.; Stiebig, H. Photoresponse enhancement in the near infrared wavelength range of ultrathin amorphous silicon photosensitive devices by integration of silver nanoparticles. *Appl. Phys. Lett.* **2009**, *95*, 033505. [\[CrossRef\]](#)
- Amanmadov, A.; Durdyev, R.; Kotyrov, M.; Melebaev, D. Synthesis of gold nanoparticles via citrate reduction and their characterization. *Eurasian Union Sci.* **2019**, *12*, 34–42. [\[CrossRef\]](#)
- Spitzer, W.G.; Mead, C.A. Barrier Height Studies on Metal-Semiconductor Systems. *J. Appl. Phys.* **1963**, *34*, 3061–3069. [\[CrossRef\]](#)
- Mead, C.A.; Spitzer, W.G. Conduction band minima at AlAs and AlSb. *Phys. Rev. Lett.* **1963**, *11*, 358–361. [\[CrossRef\]](#)
- Spitzer, W.G.; Mead, C.A. Conduction Band Minima of Ga(As_{1-x}P_x). *Phys. Rev.* **1964**, *133*, A872–A875. [\[CrossRef\]](#)
- Spitzer, W.G.; Gershenson, M.; Frosch, C.J.; Gibbs, D.E. Optical absorption in n-type gallium phosphide. *J. Phys. Chem. Sol.* **1959**, *11*, 339–341. [\[CrossRef\]](#)

27. Davydov, R.; Davydov, V.; Dudkin, V. The Nuclear Magnetic Flowmeter for Monitoring the Consumption and Composition of Oil and Its Complex Mixtures in Real-Time. *Energies* **2022**, *15*, 3259. [[CrossRef](#)]
28. Mikhailova, M.P.; Moiseev, K.D.; Yakovlev, Y.P. Discovery of III–V Semiconductors: Physical Properties and Application. *Semiconductors* **2019**, *53*, 273–290. [[CrossRef](#)]
29. Aspnes, D.E.; Studna, A.A. Dielectric functions and optical parameters of Si, Ge, GaP, GaAs, GaSb, InP, InAs and InSb from 1.5 to 6.00 eV. *Phys. Rev. B* **1983**, *27*, 985–1009. [[CrossRef](#)]
30. Hedges, R.C.; Zipperian, T.E.; Dawson, L.R.; Biefeld, R.M.; Walko, R.J.; Dvorak, A.M. Gallium phosphide junctions with low leakage for energy conversion and near ultraviolet detectors. *J. Appl. Phys.* **1991**, *69*, 6500–6505.
31. Seredin, P.V.; Goloshchapov, D.L.; Arsenyev, I.N.; Nikolaev, D.N.; Pikhtin, N.A.; Slipchenko, S.O. Spectroscopic Studies of Integrated GaAs/Si Heterostructures. *Semiconductors* **2021**, *55*, 44–50. [[CrossRef](#)]
32. Diuldin, M.V.; Melebayew, D.; Terukov, E.; Hogland, W.; Kosolapov, V.M.; Bobyl, A.V.; Pashikova, T.D.; Garadzha, N.; Shamuhammedowa, M. Highly sensitive photodetectors on the basis of Au-oxide-n-GaP_{0.4}As_{0.6}. In *IOP Conference Series: Earth and Environmental Science*; IOP Publishing: Bristol, UK, 2022; Volume 1096, p. 012005.
33. Davydov, R.; Antonov, V.; Makeev, S.; Batov, Y.; Dudkin, V.; Myazin, N. New high-speed system for controlling the parameters of a nuclear reactor in a nuclear power plant. In Proceedings of the E3S Web of Conferences, St. Petersburg, Russia, 25–27 June 2019; Volume 140, p. 02001.
34. Davydov, R.; Antonov, V.; Angelina, M. Parameter Control System for a Nuclear Power Plant Based on Fiber-Optic Sensors and Communication Lines. In Proceedings of the 2019 IEEE International Conference on Electrical Engineering and Photonics, EExPolytech, St. Petersburg, Russia, 17–18 October 2019; pp. 42–45.
35. Boudjemila, L.; Krasnoshchekov, V.; Olimov, S.; Diuldin, M.; Kasimakhunova, A. Some features of photoelectrical properties of highly efficient solar cells based on Si. In Proceedings of the 2020 IEEE International Conference on Electrical Engineering and Photonics, EExPolytech, St. Petersburg, Russia, 15–16 October 2020; pp. 223–226.
36. Rud, Y.V. Photopleochroism and the physical principles of the preparation of semiconductor polarimetric photodetectors. *Sov. Phys. J.* **1986**, *29*, 638–650. [[CrossRef](#)]
37. Murat, S.; Fahrettin, Y. Photovoltaic and interface state density properties of the Au/n-GaAs Schottky barrier solar cell. *Thin Solid Film.* **2011**, *519*, 1950–1954.
38. Stirn, R.J.; Yeh, Y.C.M. A 15% efficient antireflectioncoated metal-oxide-semiconductor solar cell. *Appl. Phys. Lett.* **1975**, *27*, 95–98. [[CrossRef](#)]
39. Rud, V.Y.; Rud, Y.V.; Terukov, E.I. Polarization studies of the photoelectric properties of II–IV–V₂-semiconductor-compound–electrolyte systems. *J. Opt. Technol.* **2016**, *83*, 275–278. [[CrossRef](#)]
40. Rud, V.; Melebaev, D.; Trapeznikova, I.; Diuldin, M.; Yakusheva, M.; Bykova, N. Features of Metal Dielectric Structures Based on GaP with Avalanche Multiplication Effect. In Proceedings of the 2022 International Conference on Electrical Engineering and Photonics (EExPolytech), St. Petersburg, Russia, 20–21 October 2022; pp. 379–382.

Disclaimer/Publisher’s Note: The statements, opinions and data contained in all publications are solely those of the individual author(s) and contributor(s) and not of MDPI and/or the editor(s). MDPI and/or the editor(s) disclaim responsibility for any injury to people or property resulting from any ideas, methods, instructions or products referred to in the content.